Check for updates

Received: 5 February 2019 | Revised: 15 October 2019 | Accepted: 21 November 2019

DOI: 10.1111/gcb.14965

PRIMARY RESEARCH ARTICLE

Global Change Biology WILEY

Sea ice loss increases genetic isolation in a high Arctic ungulate metapopulation

Bart Peeters[1] | Mathilde Le Moullec[1] | Joost A. M. Raeymaekers[2] | Jonatan F. Marquez[1] | Knut H. Røed[3] | Åshild Ø. Pedersen[4] | Vebjørn Veiberg[5] | Leif Egil Loe[6] | Brage B. Hansen[1]

[1]Centre for Biodiversity Dynamics, Department of Biology, Norwegian University of Science and Technology, Trondheim, Norway

[2]Faculty of Biosciences and Aquaculture, Nord University, Bodø, Norway

[3]Department of Basic Sciences and Aquatic Medicine, Norwegian University of Life Sciences, Oslo, Norway

[4]Norwegian Polar Institute, Fram Centre, Tromsø, Norway

[5]Norwegian Institute for Nature Research, Trondheim, Norway

[6]Department of Ecology and Natural Resource Management, Norwegian University of Life Sciences, Ås, Norway

Correspondence
Bart Peeters, Centre for Biodiversity Dynamics, Department of Biology, Norwegian University of Science and Technology, NO-7491 Trondheim, Norway.
Email: bart.peeters@ntnu.no

Funding information
Svalbard Environmental Protection Fund, Grant/Award Number: 14/137 and 15/105; Research Council of Norway, Grant/Award Number: 223257, 244647, 235652, 246054, 257173 and 276080; Norwegian Polar Institute

Abstract

Sea ice loss may have dramatic consequences for population connectivity, extinction–colonization dynamics, and even the persistence of Arctic species subject to climate change. This is of particular concern in face of additional anthropogenic stressors, such as overexploitation. In this study, we assess the population-genetic implications of diminishing sea ice cover in the endemic, high Arctic Svalbard reindeer (*Rangifer tarandus platyrhynchus*) by analyzing the interactive effects of landscape barriers and reintroductions (following harvest-induced extirpations) on their metapopulation genetic structure. We genotyped 411 wild reindeer from 25 sampling sites throughout the entire subspecies' range at 19 microsatellite loci. Bayesian clustering analysis showed a genetic structure composed of eight populations, of which two were admixed. Overall population genetic differentiation was high (mean F_{ST} = 0.21). Genetic diversity was low (allelic richness [AR] = 2.07–2.58; observed heterozygosity = 0.23–0.43) and declined toward the outer distribution range, where populations showed significant levels of inbreeding. Coalescent estimates of effective population sizes and migration rates revealed strong evolutionary source–sink dynamics with the central population as the main source. The population genetic structure was best explained by a landscape genetics model combining strong isolation by glaciers and open water, and high connectivity by dispersal across winter sea ice. However, the observed patterns of natural isolation were strongly modified by the signature of past harvest-induced extirpations, subsequent reintroductions, and recent lack of sea ice. These results suggest that past and current anthropogenic drivers of metapopulation dynamics may have interactive effects on large-scale ecological and evolutionary processes. Continued loss of sea ice as a dispersal corridor within and between island systems is expected to increase the genetic isolation of populations, and thus threaten the evolutionary potential and persistence of Arctic wildlife.

KEYWORDS

Arctic, circuit theory, climate change, extinction risk, harvesting, isolation, landscape genetics, least-cost path, population genetics, sea ice

This is an open access article under the terms of the Creative Commons Attribution-NonCommercial License, which permits use, distribution and reproduction in any medium, provided the original work is properly cited and is not used for commercial purposes.
© 2019 The Authors. *Global Change Biology* published by John Wiley & Sons Ltd

1 | INTRODUCTION

Many current threats to biodiversity are linked to anthropogenic stressors, which have either direct (e.g., through exploitation) or indirect (e.g., through habitat fragmentation, climate change) effects on populations (Lande, 1998). Direct effects of overharvesting on population demography can have long-term evolutionary consequences through loss of genetic diversity, changes in population subdivision, or selective genetic changes (Allendorf, England, Luikart, Ritchie, & Ryman, 2008; Pinsky & Palumbi, 2014). Such genetic effects can reduce the evolutionary potential, delay population recovery and increase extinction risk (Frankham, 2005). In the Arctic, mammals such as the polar bear (*Ursus maritimus*), bowhead whale (*Balaena mysticetus*), walrus (*Odobenus rosmarus*), Arctic fox (*Vulpes lagopus*), and caribou and reindeer (*Rangifer tarandus*) have been extensively harvested in the past (Fay, Kelly, & Sease, 1989; Higdon, 2010; Kruse, 2017), but genetic impact studies have so far been rare (Alter et al., 2012; Petersen, Manseau, & Wilson, 2010; Taylor, Jenkins, & Arcese, 2012). Furthermore, global warming strongly influences the Arctic ecosystem, and is expected to increasingly affect future ecological dynamics (Descamps et al., 2017; Post et al., 2009, 2013).

A dominant feature of Arctic climate change is the rapid loss of sea ice, with far-reaching ecological implications (Post et al., 2013; Stroeve, Holland, Meier, Scambos, & Serreze, 2007). Sea ice provides an important corridor for dispersal across water bodies in Arctic fox (Geffen et al., 2007; Norén et al., 2011), polar bear (Laidre et al., 2018), caribou (Jenkins et al., 2016; Leblond, St-Laurent, & Côté, 2016; Miller, Barry, & Calvert, 2005), and even vascular plants (Alsos et al., 2016). Because sea ice loss is associated with increased global temperatures and Arctic amplification (Serreze, Barrett, Stroeve, Kindig, & Holland, 2009), a future increase in the isolation of Arctic island populations is expected. In general, island populations have lower genetic diversity and higher levels of inbreeding than mainland populations (Frankham, 1997, 1998). This makes them more prone to loss of genetic diversity through genetic drift and, ultimately, increased extinction risk following environmental perturbations (Frankham, 1998; Lande, 1998; Saccheri et al., 1998). Dispersal and recolonization facilitated by sea ice are therefore crucial for the persistence and resilience of many Arctic island populations (Hanski, 1998; Post et al., 2013; Vuilleumier, Bolker, & Leveque, 2010).

Svalbard reindeer (*R. t. platyrhynchus*) live in a pristine archipelagic environment with very little human infrastructure and a simple food-web system where predation and interspecific competition are virtually absent (Descamps et al., 2017). Many reindeer populations were extirpated (i.e., locally extinct) due to overharvesting between the 17th and early 20th century (Kruse, 2017; Lønø, 1959). Today, Svalbard reindeer have largely recovered their historical range through natural recolonization and human-mediated reintroductions (Le Moullec, Pedersen, Stien, Rosvold, & Hansen, 2019). Their distribution is fragmented into semi-isolated populations by natural landscape barriers such as glaciers, steep mountains, fjords, and open water. Sea ice and fjord ice may provide an important dispersal corridor during winter (Hansen, Aanes, & Sæther, 2010; Jenkins et al., 2016; Leblond et al., 2016). However, warm water brought by the North Atlantic Current often restricts sea ice formation in southern and western parts of Svalbard (Nilsen, Skogseth, Vaardal-Lunde, & Inall, 2016), and a strong negative trend in sea ice cover over the past few decades has been reported for northern parts (Onarheim, Smedsrud, Ingvaldsen, & Nilsen, 2014). Overall, spatiotemporal variation in sea ice connectivity is likely an important driver of metapopulation dynamics and genetics in Svalbard reindeer (cf. Peary caribou *R. t. pearyi*; Jenkins et al., 2016; Mallory & Boyce, 2019), along with dispersal barriers on land and extinction–colonization dynamics linked to past overharvesting and recent reintroductions.

To better understand the ecological and evolutionary consequences of past and current anthropogenic impacts, and with particular emphasis on the potential consequences of sea ice loss, we adopted a landscape genetics approach using neutral markers in Svalbard reindeer. Landscape genetics have been extensively used to infer knowledge about the effects of landscape barriers and habitat fragmentation (Storfer, Murphy, Spear, Holderegger, & Waits, 2010), including in caribou and reindeer (Jenkins et al., 2016; Yannic et al., 2017). By sampling individuals across the entire distribution range of Svalbard reindeer, we covered a gradient of sea ice cover frequencies and landscape fragmentation through glacial and open water barriers. We were able to assess causes and consequences of extinction–colonization dynamics by including populations that persisted past overexploitation and populations in areas that were recolonized—either through natural expansion or reintroduction by humans—after harvest-induced extirpation. In particular, we expected that sea ice would represent an important dispersal corridor explaining significant parts of the reindeer's genetic differentiation and structure, potentially modified by harvest-induced extirpations and subsequent reintroduction programs.

2 | MATERIALS AND METHODS

2.1 | Study area and species

The Svalbard archipelago is located in the Arctic Ocean north of Norway (76°–81°N, 10°–35°E; Figure 1a). The largest island is Spitsbergen, followed by Nordaustlandet, Edgeøya, and Barentsøya. The landscape has a highly heterogeneous topography with coastal plains, mountain plateaus, steep slopes, wide valleys, and fjords. About 60% of the land surface is glaciated and only 15% is covered with vegetation, mainly characterized by snowbed communities, *Dryas* tundra, and sparse pioneer vegetation (Johansen, Karlsen, & Tømmervik, 2012). The northward inflow of warm Atlantic water leads to a milder climate and less sea ice along the west coast of Spitsbergen compared to the eastern parts of Svalbard, which are characterized by cold Arctic water. Sea ice concentration usually reaches its maximum in March–April, but has been gradually

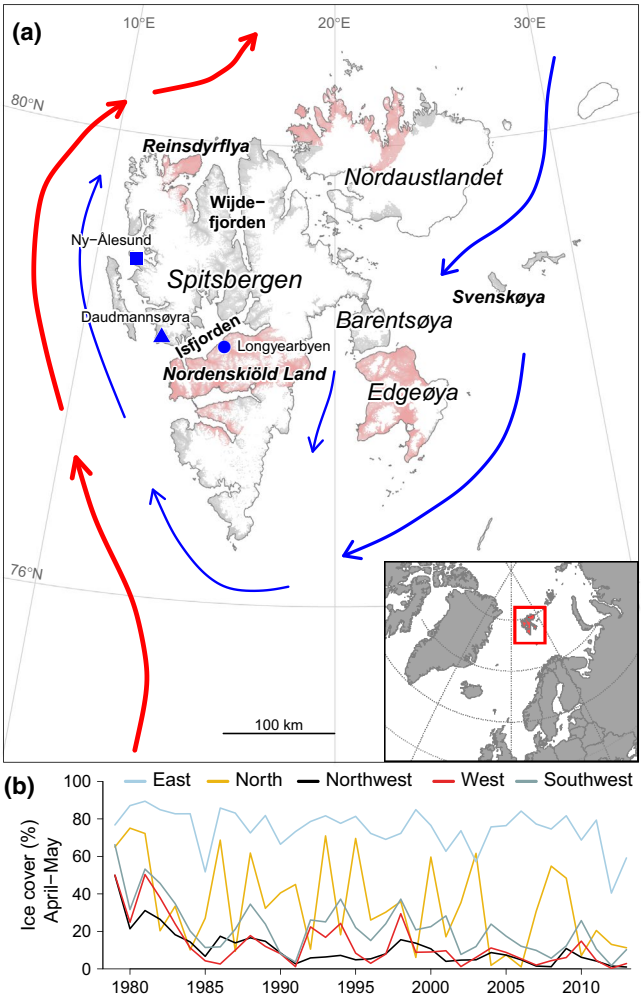

FIGURE 1 The Svalbard archipelago (a) is situated in the Arctic Ocean north of Norway (inset). Svalbard reindeer were nearly extinct due to overharvesting, but four extant populations remained (pink areas indicate known distribution in the 1950s; Lønø, 1959). Reindeer were reintroduced from the population near Longyearbyen (blue circle) to west Spitsbergen near Ny-Ålesund in 1978 (blue square) and Daudmannsøyra in 1984–1985 (blue triangle). Today, reindeer are distributed across Svalbard, except in glaciated areas (white). Coastal currents are characterized by southward cold Arctic water in the east (blue arrows) and northward warm Atlantic water in the west (red arrows). (b) Time series of April–May sea ice cover in five coastal areas of Spitsbergen (data retrieved from Prop et al., 2015)

declining from 43% to 19% cover on average across Spitsbergen during the period 1979–2013 (Figure 1b; Prop et al., 2015).

The Svalbard reindeer has very low genetic variation compared to other *Rangifer* subspecies (Cronin, Patton, Balmysheva, & MacNeil, 2003; Kvie et al., 2016; Røed, 2003; Yannic et al., 2014). Genetic differentiation has been found between populations only 45 km apart in Spitsbergen (Côté et al., 2002), likely because of their sedentary behavior, low dispersal rates, and lack of seasonal migrations (Hansen et al., 2010; Tyler & Øritsland, 1989). Svalbard reindeer became protected from harvesting in 1925 when the total population size had decreased dramatically and reindeer were extirpated across large parts of their historical range. According to Lønø (1959), only four isolated populations remained in the following parts of Svalbard (Figure 1a): Nordaustlandet (estimated population size anno 1958: N = 300–400), Edgeøya in East Svalbard (N = 500–800), Reinsdyrflya in North Spitsbergen (N = 200–300), and Nordenskiöld Land in Central Spitsbergen (N≈200). Since then, populations have gradually increased in size and expanded. At present, the subspecies has largely recovered to its pre-harvesting distribution range, although some areas show still signs of ongoing recovery (Le Moullec et al., 2019). This recovery was facilitated by translocations of individuals from the population near Longyearbyen, Nordenskiöld Land, to the west coast of Spitsbergen near Ny-Ålesund in 1978 (15 individuals; Aanes, Sæther, & Øritsland, 2000) and Daudmannsøyra in 1984–1985 (12 individuals; Governor of Svalbard, 2009; Figure 1a). Current management on Svalbard aims to conserve natural populations with minimal human interference. However, recreational hunting is allowed in a few designated areas, mainly in Nordenskiöld Land, but the hunting level is low (<5% of the local population) and has no significant impact on the population dynamics (Stien et al., 2012).

2.2 | Sampling

Samples from 456 reindeer were collected at 25 sites across the entire Svalbard archipelago (Table S1). Dispersal between nearby sampling sites was assumed to be limited by mountains, glaciers, fjords, and/or open sea and was confirmed by genetic differentiation analyses (see below). All samples were obtained between 2014 and 2016, except for nine blood samples from Nordaustlandet that were collected in 1995 and included to increase sample size in this remote location (Kvie et al., 2016).

The collected material included soft tissue (n = 104), bone (n = 66), antler (n = 69), blood (n = 9; Kvie et al., 2016), or tooth (n = 5) samples from carcasses, and fresh feces (n = 48) from live reindeer. Additionally, we obtained hair (n = 85) or soft tissue (n = 70; obtained from ear punches during ear-tagging) from live reindeer included in mark-recapture programs (Albon et al., 2017). Mark-recapture studies followed ethical requirements approved by the Norwegian Food Safety Authority. Hair, bone, antler, and tooth samples were dry-stored, fecal samples were directly stored in 96% ethanol or frozen, while soft tissue and blood samples were frozen after collection. Coordinates were recorded for all individuals at the time of sampling, except for those from Wijdefjorden and the nine individuals from Nordaustlandet sampled in 1995. For those, approximate coordinates were obtained based on sampling location descriptions.

After excluding samples with a low DNA amplification success (see below), the total dataset comprised 411 genotyped individuals covering the full geographic range of Svalbard reindeer, with sample sizes ranging from 20 to 52 individuals in eight sites, 6 to 19 individuals in eleven sites, and 1 to 4 individuals in six sites (Table S1).

2.3 | DNA extraction and microsatellite genotyping

DNA was extracted using the Chelex 100 method for hair samples (Walsh, Metzger, & Higuchi, 1991) and the spin column method (QIAGEN) for all other sample types (see Methods S1 for detailed procedures). Individuals were genotyped at 19 polymorphic microsatellite loci (Table S2) using standard procedures for PCR, electrophoresis, and quality control. For 45 samples (i.e., 6% of soft tissue samples, 1% of hair samples, 19% of feces samples, 29% of bone samples, 7% of antler samples, and 20% of tooth samples), less than 10 loci could be amplified, probably due to PCR inhibitors or low reindeer-specific DNA yield. These samples were therefore excluded. Overall, of the 411 genotyped individuals, 81% were genotyped at 19 microsatellite loci, 8% at 18 loci, 4% at 17 loci, 2% at 16 loci, and the remaining 5% at 10–15 loci. The final dataset of 411 multilocus genotypes reached a data completeness of more than 96%.

2.4 | Population genetic structure

We were interested in the population genetic structure of Svalbard reindeer at two hierarchical levels. First, we quantified genetic differentiation by calculating the global and pairwise F_{ST} (Weir & Cockerham, 1984) between all sampling sites with >5 sampled individuals (n = 18 sites; Table S3; note that one site with eight samples was excluded due to mixed cluster results; see below). F_{ST} values were tested for significance based on 10,000 permutations among samples using the R-package *strataG* (Archer, Adams, & Schneiders, 2017) in R version 3.5.1 (R Core Team, 2016). Second, to reveal large-scale patterns of genetic diversity, isolation, and connectivity, we identified populations based on a higher-order (hierarchical) genetic structure. For this, we used the individual-based Bayesian clustering analyses as implemented in *STRUCTURE* 2.3 (Pritchard, Stephens, & Donnelly, 2000) and *TESS* 2.3 (Chen, Durand, Forbes, & Francois, 2007; see Methods S2 for technical details). *STRUCTURE* performs well for inferring the number of clusters without prior knowledge of sampling locations (Latch, Dharmarajan, Glaubitz, & Rhodes, 2006). However, the joint analysis of genetic and geographic structure, as implemented in *TESS*, is expected to yield more realistic cluster assignments for individuals from weakly differentiated but distant populations (Chen et al., 2007). We then assigned individuals to their most likely cluster based on a proportional assignment threshold of ≥0.75 (see Yannic et al., 2016, for a similar approach) and, for each sampling site, calculated the proportion of individuals assigned to each cluster (Table S4). Populations could thus be delineated based on both genetic structure and geographic segregation of sampling sites.

As a conservative measure, sites with ≤5 samples as well as sites with ≤10 samples showing strong genetic admixture were hereafter only included in individual-based analyses. Genetic differentiation between populations was estimated using pairwise F_{ST} values as for sampling sites. To account for consequences of recent reintroductions on the genetic structure, we conducted a post hoc analysis in STRUCTURE excluding individuals from reintroduced sites (Figure S2). Finally, the geographic range of genetically distinct populations is of practical interest for the future management of Svalbard reindeer. To determine these ranges, we first plotted individual coordinates on the map and interpolated the individual clustering assignments (as identified with TESS) using thin plate spline regressions in the R-package *fields* (Nychka, Furrer, Paige, & Sain, 2017). The geographic range of each population was then delineated using minimum convex polygons in the R-package *adehabitatHR* (Calenge, 2006).

2.5 | Genetic diversity analyses

Analyses of genetic diversity were performed at the sampling site and population level, but only reported for populations in the main text (see Table S1 for genetic diversity estimates of sampling sites). Genetic diversity was assessed by measures of AR and heterozygosity. AR and private AR (i.e., alleles unique to the population; AR_P) were calculated using a rarefaction approach on a minimum sample size of 34 genes (i.e., 17 diploid individuals) implemented in *HP-RARE* 1.1 (Kalinowski, 2005). Observed and unbiased expected heterozygosity (H_O and uH_E) were calculated and averaged over loci using the R-package *hierfstat* (Goudet, 2005). Differences in observed and expected heterozygosity between populations at the locus level were tested using two-tailed, paired sample t tests after arcsine square root transformation (e.g., Côté et al., 2002). Similarly, a non-parametric Mann–Whitney U test was used to test for differences in AR. Inbreeding coefficients (F_{IS}) were calculated in *hierfstat* and bootstrapped using 10,000 iterations to obtain 95% confidence intervals.

Individual heterozygosity was estimated as the proportion of heterozygous loci for all 411 genotyped individuals (Coulon, 2010), which was then spatially interpolated using a thin plate spline regression in the R-package *fields* (Nychka et al., 2017). We tested for an expected decrease in individual heterozygosity toward the range margin (Eckert, Samis, & Lougheed, 2008) using a generalized linear regression model (binomial family with logit link function) with the Euclidian distance between individual coordinates and the reindeer density-weighted range center (Le Moullec et al., 2019) as a predictor. We also used a generalized mixed regression model to correct for non-independence among individuals from the same sampling site (n = 25).

2.6 | Effective population sizes and gene flow

To investigate metapopulation dynamics over an evolutionary timescale, we estimated long-term mutation-scaled effective population sizes (θ) and directional gene flow between populations using a coalescent approach in *Migrate-n* 3.6.11 (Beerli, 2006; Beerli & Felsenstein, 2001; Methods S3; Table S5). Here, individuals from reintroduced sites and admixed populations were excluded to avoid spurious estimates of coalescent effective population size and gene flow.

Contemporary effective population sizes (N_e) were estimated using the linkage disequilibrium method in *NeEstimator* 2.0 (Do et al., 2014). As bias and precision of this method depend on the criterion of screening out rare alleles (Waples & Do, 2010), we estimated N_e using alleles with frequencies >0.02 and >0.01. To estimate ratios of N_e/N_c, we obtained estimates of census population size (N_c) and density (N_d) through distance sampling monitoring surveys conducted across Svalbard from 2013 to 2016 (Le Moullec et al., 2019). In further details, reindeer abundance was predicted at the pixel level (250 × 250 m) from a density surface model (Miller, Burt, Rexstad, & Thomas, 2013) where vegetation productivity index (maximum Normalized Difference Vegetation Index) was the main driver. Comparison of N_e estimates and N_e/N_c ratios clearly indicated that the point estimate of N_e in one population was inflated when using allele frequencies >0.02 (Table S6). We therefore only report N_e based on allele frequencies >0.01 in the main text. Directional estimates of recent gene flow (i.e., over the last few generations) were estimated using *BayesAss* 3.0.4 (Wilson & Rannala, 2003) for all populations (Methods S3; Table S7).

2.7 | Landscape genetics analysis

To better understand how gene flow in this fragmented metapopulation was affected by landscape barriers (glaciers, open sea, and mountains) and a seasonally dynamic corridor (winter sea ice), we investigated patterns of isolation-by-distance (IBD) and isolation-by-resistance (IBR). Landscape genetics were primarily analyzed at the sampling site level due to the discontinuous distribution and sedentary behavior of Svalbard reindeer (Côté et al., 2002) and the strong genetic differentiation observed among sampling sites (Table S3). Genetic distances among sites were estimated as $F_{ST}/(1 - F_{ST})$; Rousset, 1997). Landscape distances were obtained by averaging distances among individuals between pairs of sampling sites, which were calculated as Euclidian distances (IBD; hereafter referred to as geographic distances) and ecological distances derived from resistance maps (IBR; see below). Genetic distances among individuals were estimated as Rousset's $\hat{a}$ (Rousset, 2000) using the program *SPAGeDi* 1.5 (Hardy & Vekemans, 2002) to analyze landscape genetics at the individual level.

Ecological distances (IBR) were estimated using both least-cost path and circuit theoretic models on resistance surfaces (McRae & Beier, 2007) in the R-package *gdistance* (Van Etten, 2017; see Methods S4 for technical details). Least-cost paths estimate the optimal route between positions, assuming perfect knowledge of the landscape, whereas circuit theory simultaneously considers all possible pathways connecting pairs of individuals/sites (McRae, 2006; McRae & Beier, 2007). Conductance values ($0 < c < 1$) were used to assign low to high probabilities of dispersal across different types of landscape surface (slope and elevation, glaciers, open water, and sea ice). We first investigated the effects of glaciers and open water on genetic distances (IBR scenario 1), while accounting for the effects of slope and elevation on movement cost. We then expanded the landscape model of IBR scenario 1 to include the effect of sea ice (IBR scenario 2) by increasing the conductance of sea surfaces with various thresholds of sea ice frequency (minimum of 50%–99%) during March 1986–2015. A threshold of approximately 100% sea ice frequency corresponded to a landscape model including connectivity across ice only in marine areas where ice was present during March in all years between 1986 and 2015. Parameter selection of conductance values and the optimal threshold of sea ice frequency were informed by Mantel correlations (Mantel, 1967) between genetic and ecological distances among natural sites (i.e., excluding sampling sites of reintroduced origin; Figures S3 and S4).

To understand the effects of reintroductions on landscape genetics, we separately analyzed IBD and IBR for genetic distances among natural sites (n = 13 sites) and genetic distances between reintroduced sites (n = 5 sites) and natural sites of either source (n = 4 sites) or non-source (n = 9 sites) origin of reintroductions (Table S1). However, due to the high computational workload to estimate circuit theory distances (see Methods S4), we only investigated the relationship between genetic distance and circuit theory distance at the natural site level. Landscape genetics at the individual level were analyzed for IBD and least-cost path IBR using the same conductance values and threshold of winter sea ice frequency as obtained from landscape genetics at the sampling site level.

Mantel tests between genetic and landscape distances were performed using the R-package *vegan* (Oksanen et al., 2018), but IBD versus IBR was tested using maximum-likelihood population effects models (MLPE) for final inference (Clarke, Rothery, & Raybould, 2002). The mixed effects parameterization in MLPE accounted for non-independence among the pairwise data. We implemented MLPE using the R-package *ResistanceGA* (Peterman, 2018), but only for analyses among natural sites as MLPE could not handle the incomplete distance matrices of pairwise combinations between natural and reintroduced sites. Marginal and conditional R^2 (i.e., variance explained by fixed effects only and both fixed and random effects, respectively) were estimated using the R-package *piecewiseSEM* (Lefcheck, 2016). Model selection was informed by Akaike's information criterion corrected for sample size (AIC_c).

3 | RESULTS

3.1 | Population genetic structure

STRUCTURE revealed a strong genetic structure characterized by three major clusters and a further subdivision into six clusters (Figure 2a; Figure S1). The analysis in *TESS* confirmed the maximal number of six clusters (Figure 2; Figure S1). A clear composition of sampling sites from the same region was evident for each genetic cluster, with minimum 60%, but typically >80% of individuals in each site assigned to one cluster (Table S4). Furthermore, the strong genetic structure of both the individual-based analyses (Figure 2) and pairwise genetic differentiation among sampling sites (Table S3) strongly reflected the geographic segregation of

sampling sites. However, two sampling sites with ≥10 sampled individuals, Wijdefjorden and North Isfjorden, showed a high degree of admixture (<60% of individuals assigned to one cluster).

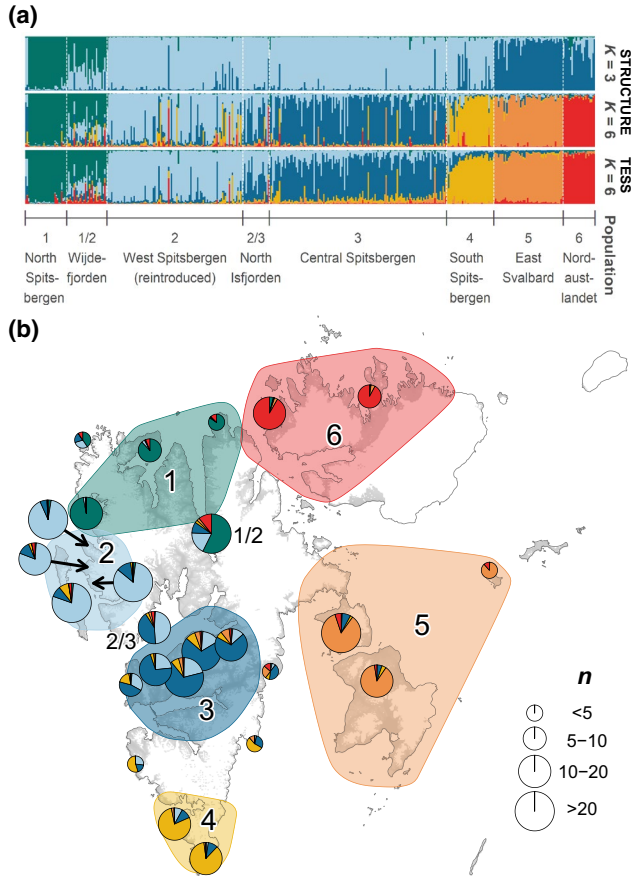

FIGURE 2 Bayesian clustering analyses revealed three major clusters (K = 3) and a further subdivision into six clusters (K = 6). (a) Individual cluster assignments (q [0, 1]) for 411 Svalbard reindeer in STRUCTURE (K = 3 and 6) and TESS (K-max = 6), ordered in a south- and eastward direction by population. (b) Genetic structure at 25 sampling sites based on K = 6 in TESS (pie charts increasing in size relative to number of sampled individuals n). Cluster ranges were estimated using minimum convex polygons after spatial interpolation of individual clustering assignments

Individuals and sampling sites were accordingly delineated into eight populations, that is, six separate populations for each of the six genetic clusters (North Spitsbergen, West Spitsbergen, Central Spitsbergen, South Spitsbergen, East Svalbard, and Nordaustlandet) and two populations showing mixed genetic cluster origins (Wijdefjorden and North Isfjorden). Note that a large proportion of individuals (0.45–0.50 per sampling site; Table S4) from Central Spitsbergen were admixed between Central Spitsbergen and West Spitsbergen cluster. This suggests a founder bottleneck and genetic drift after individuals were translocated from Central Spitsbergen to West Spitsbergen (Aanes et al., 2000). The post hoc analysis excluding the reintroduced sites supported the delineation of Central Spitsbergen as a distinct (rather than an admixed) population (Figure S2). The recolonized Wijdefjorden population indicated strong admixture with genetic signals from North and West Spitsbergen, while the post hoc analysis also supported the delineation of Wijdefjorden as a separate population (Figure S2). Finally, the mixed genetic signature in North Isfjorden and complementary analysis of recent gene flow (Table S7) suggested a recolonization from Central Spitsbergen and the reintroduced site at Daudmannsøyra (Figure 1a).

Global F_{ST} was 0.21 ± 0.09, while pairwise F_{ST} between populations ranged from 0.05 (North Isfjorden–Central Spitsbergen) to 0.37 (North Spitsbergen–Nordaustlandet; Table 1). North Spitsbergen was the most strongly differentiated population (F_{ST} > 0.31, except when paired with Wijdefjorden). The population of reintroduced origin, West Spitsbergen, and its source, Central Spitsbergen, were significantly differentiated from each other. The admixed North Isfjorden population was also significantly differentiated from West and Central Spitsbergen. Finally, pairwise F_{ST} values between sites supported the expectation that gene flow was limited due to landscape barriers (Table S3).

3.2 | Genetic diversity

We found 73 alleles at the 19 microsatellite loci, with a range of two to seven alleles per locus (Table S2). AR of populations

TABLE 1 Pairwise genetic differentiation (F_{ST}) among the eight populations. Wijdefjorden and North Isfjorden were identified as admixed populations

Population	North Spitsbergen	Wijdefjorden	West Spitsbergen	North Isfjorden	Central Spitsbergen	South Spitsbergen	East Svalbard	Nordaustlandet
North Spitsbergen								
Wijdefjorden	0.158							
West Spitsbergen	0.342	0.144						
North Isfjorden	0.370	0.194	0.084					
Central Spitsbergen	0.317	0.163	0.064	0.051				
South Spitsbergen	0.361	0.164	0.123	0.222	0.134			
East Svalbard	0.370	0.277	0.197	0.188	0.158	0.262		
Nordaustlandet	0.374	0.207	0.166	0.215	0.160	0.198	0.219	

Note: All F_{ST} values were significantly different from zero after Bonferonni correction based on 10,000 permutations among samples.

TABLE 2 Genetic diversity and population size estimates of the eight populations. Wijdefjorden and North Isfjorden were identified as admixed populations

Population	*n*	AR	AR_P	AR_{P_sub}	H_O	uH_E	F_{IS} (95% CI)	$N_c \pm SE$	N_d	N_e (95% CI)
North Spitsbergen	27	2.07	0.04	0.20	0.24	0.30	**0.19 (0.08; 0.28)**	2,678 ± 400	1.84	36.2 (11.1; ∞)
Wijdefjorden	29	2.58	0.01	–	0.37	0.39	0.03 (−0.08; 0.17)	572 ± 81	1.97	219.9 (36.3; ∞)
West Spitsbergen	98	2.42	0.01	0.02	0.33	0.35	**0.07 (0.02; 0.13)**	1,887 ± 241	2.88	100.2 (47.8; 437.9)
North Isfjorden	19	2.45	0.01	–	0.35	0.38	0.09 (−0.03; 0.19)	1,730 ± 184	2.87	38.5 (13.5; ∞)
Central Spitsbergen	119	2.55	0.02	0.07	0.43	0.43	0.00 (−0.05; 0.05)	5,581 ± 650	2.97	221.1 (106.1; 1593.1)
South Spitsbergen	28	2.35	0.09	0.13	0.27	0.34	**0.20 (0.02; 0.36)**	648 ± 82	2.26	21.6 (10.8; 67.2)
East Svalbard	50	2.36	0.09	0.15	0.29	0.34	**0.16 (0.07; 0.31)**	3,289 ± 1,085	1.38	108.5 (35.7; ∞)
Nordaustlandet	23	2.08	0.13	0.16	0.23	0.30	**0.25 (0.12; 0.37)**	1,922 ± 710	0.77	63.3 (14.0; ∞)

Abbreviations: AR, rarefied allelic richness averaged over loci; AR_P, rarefied allelic richness of private alleles; AR_{P_sub}, same as AR_P but estimated without admixed populations; H_O, observed heterozygosity; uH_E, unbiased expected heterozygosity; F_{IS}, inbreeding coefficient with significant estimates indicated in bold; *n*, sample size; N_c, estimated census population size with standard error (*SE*); N_d, population density (N_c/km^2); N_e, effective population size based on linkage disequilibrium with 95% jackknifed confidence intervals.

was on average 2.36 ± 0.19 and ranged from 2.07 in North Spitsbergen to 2.58 in Wijdefjorden (Table 2). Private AR (when excluding the two admixed populations) was highest in North Spitsbergen, with approximately 10% of the estimated AR being unique to this population (calculated as the ratio of AR_{P_sub} to AR; Table 2). Similarly, 6%–8% of *AR* was unique to South Spitsbergen, East Svalbard, and Nordaustlandet. Observed heterozygosity within populations was on average 0.31 ± 0.07 and ranged from 0.23 to 0.43 in Nordaustlandet and Central Spitsbergen, respectively (Table 2). Differences in *AR* and expected heterozygosity between loci were not statistically significant after Bonferroni correction for multiple comparisons. However, observed heterozygosity was significantly higher in Central Spitsbergen than East Svalbard (paired $t_{18} = 3.74$; $p < .01$) and Nordaustlandet (paired $t_{18} = 4.30$; $p < .001$), and also significantly higher in Central Spitsbergen than North Spitsbergen (paired $t_{18} = 3.64$; $p < .01$) after Bonferroni correction when the two admixed populations were excluded from the multiple comparison. As such, conforming with the central-marginal hypothesis (Eckert et al., 2008), heterozygosity at the individual level was highest in Central Spitsbergen and decreased with increasing distance from the reindeer density-weighted range center (binomial regression, estimates with standard errors (±*SE*) on logit scale: intercept = −0.16 ± 0.05, slope = −0.52 ± 0.05 per 100 km from the range center; Figure 3). A mixed model correcting for non-independence among individuals from the same sampling site yielded qualitatively the same results (intercept = −0.26 ± 0.10, slope = −0.45 ± 0.08, random variance of intercept = 0.02 for *n* = 25 groups). Finally, significant levels of inbreeding were found in all peripheral populations, but not in Central Spitsbergen or the admixed populations Wijdefjorden and North Isfjorden (Table 2).

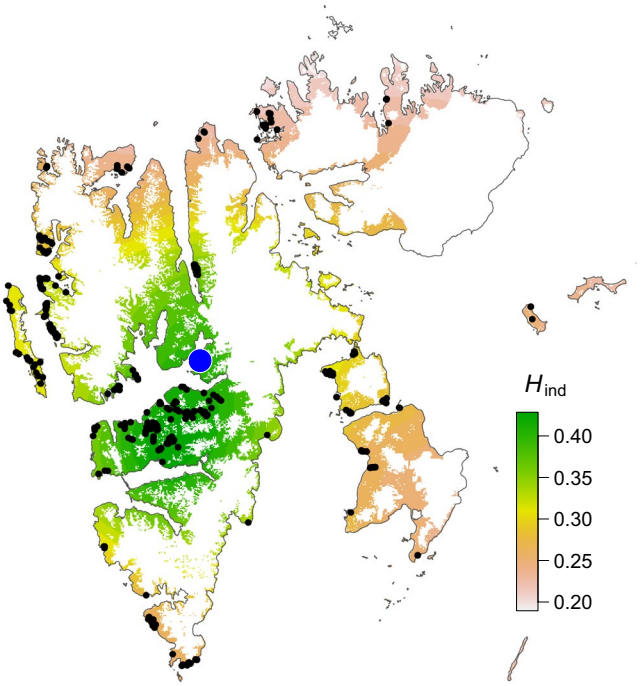

FIGURE 3 Spatial variation of individual heterozygosity (H_{ind}, i.e., the proportion of heterozygous loci in individuals based on 19 microsatellite loci) in 411 Svalbard reindeer (black dots). Estimates of individual heterozygosity were spatially interpolated using a thin plate spline regression. The density-weighted range center is indicated by the large blue dot

3.3 | Effective population sizes and gene flow

Estimates of contemporary N_e were lower than 500 in all populations, and lower than 50 in North Spitsbergen, South Spitsbergen, and North Isfjorden (Table 2). The N_e/N_c ratio was clearly highest in Wijdefjorden

(0.38) and ranged from 0.02 to 0.05 (mean ± *SD* = 0.03 ± 0.01) in all other populations. N_e increased with expected heterozygosity (Pearson's r = .74; p = .038) and AR (r = .69; p = .060), and decreased with inbreeding coefficients (r = −.78; p = .023).

The coalescent approach in *Migrate-n* revealed evolutionary source–sink dynamics with Central Spitsbergen as the major source for gene flow (Figure 4; Table S5). Significant levels of gene flow were found from Central Spitsbergen to all other populations, and from South Spitsbergen and East Svalbard to Central Spitsbergen. However, mutation-scaled migration rates were significantly higher from Central Spitsbergen to South Spitsbergen and East Svalbard than in the opposite direction. Patterns of recent gene flow indicated highest migration rates from West Spitsbergen (migration rate m = 0.09) and Central Spitsbergen (m = 0.14) to North Isfjorden, with very little migration in the opposite direction (m < 0.02; Table S7). Other estimates of recent gene flow were generally low (m < 0.05) with no clear patterns of directionality, indicating high insularity of populations during the past few generations.

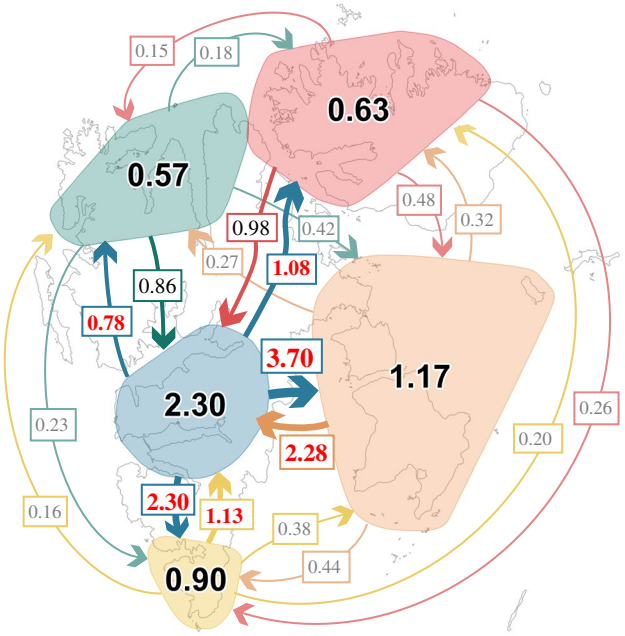

FIGURE 4 Evolutionary source–sink dynamics between five populations (i.e., excluding reintroduced and admixed populations) of Svalbard reindeer were evident from coalescent estimates of mutation-scaled effective population sizes (θ, inside polygons) and effective migrants per generation ($N_e \cdot m$, arrows with squares). Values with significant evidence for connectivity are indicated in red. The highest levels of connectivity are indicated with large, bold arrows, while faint arrows and text indicate low connectivity. All estimates are independent of geographic distances. Colors of polygons (i.e., cluster ranges) and directional arrows correspond with colors used for cluster delineation in Figure 2

3.4 | Landscape genetics

Genetic differentiation among natural sites increased with geographic distance (IBD: Table 3; Figure 5a). However, IBR explained twice the amount of variation in genetic distances than IBD when using least-cost path or circuit theory distances accounting for landscape fragmentation with low conductance for glaciers (c = 0.01) and open water (c = 0.05; IBR scenario 1: Table 3; Figure 5b,c). Models accounting for high connectivity across winter sea ice performed considerably better, especially when using circuit theory distances (IBR scenario 2: Table 3; Figure 5d,e). Mantel correlations in circuit theory and least-cost path analyses were highest for landscape models with areas covered by winter sea ice during, respectively, ≥75% and ≥99% of the time from 1986 to 2015, and using sea ice conductance values near 0.7 and 0.9, respectively (Figures S3 and S4). Therefore, genetic differentiation was not explained by IBD alone, but was strongly influenced by landscape barriers (open water and glaciers) and dispersal across winter sea ice.

Landscape distances among natural sites were intermediately correlated between IBD and circuit IBR scenario 2 (Mantel's r = .44; p = .002) and between least-cost IBR scenario 1 and circuit IBR scenario 2 (Mantel's r = .48; p < .001). All other landscape distances were strongly correlated (Mantel's r > .70; p < .001; Table S8). Partial Mantel correlations after correcting for circuit distance of IBR scenario 2 were only significant between genetic distance and least-cost distance of IBR scenario 1 (Mantel's r = .47;

TABLE 3 Results from landscape genetics analysis among natural sites of Svalbard reindeer. Mantel correlations are given for the relationship between Rousset's pairwise differentiation ($F_{ST}/(1 - F_{ST})$) and either Euclidian (IBD), least-cost path or circuit theory distances (IBR). Landscape models of IBR accounted for barrier effects (glaciers, open water, and topography) only (IBR 1), or both barrier effects and connectivity across sea ice (IBR2)

	Mantel test	MLPE			
Landscape distance	R	$\beta \pm SE$	$R^2_{marginal}$	$R^2_{conditional}$	ΔAIC_c
Circuit IBR 2	0.78***	0.161 ± 0.019	0.64	0.70	0.00
Least-cost IBR 2	0.70***	0.139 ± 0.019	0.53	0.69	4.24
Least-cost IBR 1	0.63***	0.119 ± 0.019	0.42	0.63	13.06
Circuit IBR 1	0.64***	0.116 ± 0.020	0.42	0.61	18.09
Euclidian IBD	0.48**	0.079 ± 0.018	0.20	0.52	28.59

Note: Results from maximum likelihood population effects models (MLPE) show standardized effect size (β) with standard errors (*SE*), marginal and conditional R^2, and differences in sample-size-corrected Akaike's information criterion (ΔAIC_c) from the model with lowest AIC_c.

p Values of Mantel correlations computed based on 10,000 permutations: **p < .01; ***p < .001.

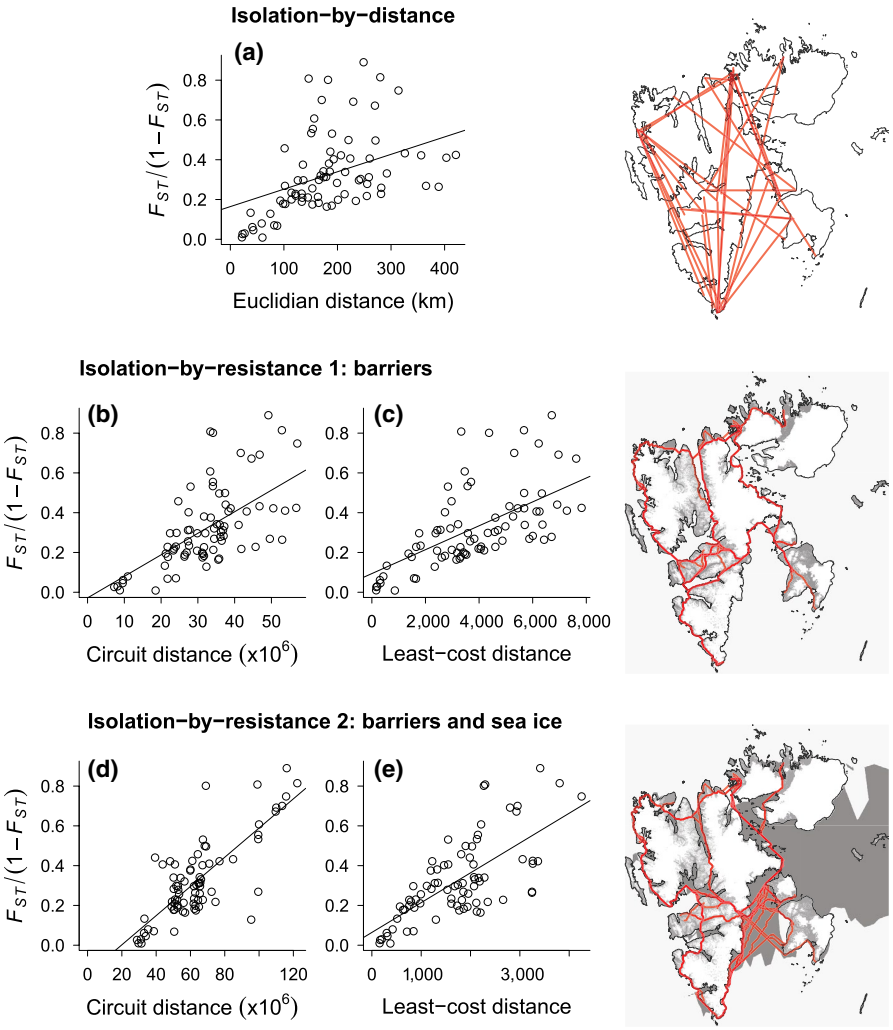

FIGURE 5 Genetic differentiation among natural sites of Svalbard reindeer was best explained by isolation-by-resistance (IBR) models accounting for landscape barriers and connectivity across winter sea ice. Relationships between genetic and geographic distances are shown for models of (a) isolation-by-distance (IBD), (b, d) IBR using circuit theory distances and (c, e) IBR using least-cost path distances. IBR scenario 1 (b, c) accounted for barrier effects of open water, glaciers, and topography, whereas IBR scenario 2 (d, e) accounted for barrier effects as well as connectivity across winter sea ice. Black lines show linear regressions from maximum-likelihood population effect models. The maps on the right illustrate connectivity and dispersal routes for the three landscape models, showing Euclidian or 'straight-line' trajectories (top map), and least-cost path trajectories (middle and bottom map) for 30 random pairs of individuals (red lines) on transitions maps with low (white) to high (dark grey) conductance. No transition map was used for IBD

p = .008). Accordingly, including both landscape distances in the same MLPE model slightly improved the explained variance of genetic distance (standardized effect size with standard errors $\beta \pm SE$: intercept = 0.334 ± 0.019, circuit IBR2 = 0.124 ± 0.017, least-cost IBR1 = 0.066 ± 0.016; R^2_{marginal} = .69; $R^2_{\text{conditional}}$ = .71). At the individual level, genetic distances among pairs of reindeer were positively correlated with geographic distances (IBD: Mantel's r = .36; p < .001; MLPE R^2_{marginal} = .22; $R^2_{\text{conditional}}$ = .44), but more strongly correlated with least-cost distances (IBR scenario 1: Mantel's r = .40; p < .001; MLPE R^2_{marginal} = .34; $R^2_{\text{conditional}}$ = .53; and IBR scenario 2: Mantel's r = .41; p < .001, MLPE R^2_{marginal} = .35; $R^2_{\text{conditional}}$ = .53; Figure S5). Note that the high statistical power arises from the high number of observations (n = 294 reindeer; 86,436 pairwise distances; Luximon, Petit, & Broquet, 2014) and that circuit distances were not computed for all pairs of individuals (Material S4).

The importance of sea ice connectivity was also evident from the strong genetic differentiation between sampling sites of North Spitsbergen and nearby reintroduced sites in West Spitsbergen, where reindeer had previously been extirpated due to overharvesting (Tables 1 and S3). When comparing these reintroduced sites with natural, non-source sites, a tendency for a negative relationship between genetic distance and landscape distance was observed (Figure S6). Such an inverse relationship suggests a lack of migration-drift equilibrium among these sites, likely related to the rare sea ice cover along the west coast in the past few decades (Figure 1b; Onarheim et al., 2014).

4 | DISCUSSION

This study demonstrates how the metapopulation genetics of an island ungulate can be shaped by a combination of landscape barriers and interactive effects of past and current anthropogenic drivers of extinction–recolonization dynamics. Whereas glaciers and open sea were clearly strong barriers to gene flow (Figure 5b,c), connectivity strongly increased in areas with frequent winter sea ice (Figure 5d,e). However, these landscape effects were modified by past conservation actions following harvest-induced extirpations, causing strong differentiation between reintroduced and natural sites over very short geographic distances. Clustering analyses resulted in a delineation of eight populations; six separate populations for each of the

six genetic clusters and two populations showing mixed cluster origins (Figure 2). Peripheral populations had lower genetic diversity, lower effective population sizes, and higher inbreeding coefficients than the central population, Central Spitsbergen (Table 2; Figure 3). Furthermore, estimates of directional gene flow based on coalescence theory suggested evolutionary source–sink dynamics with Central Spitsbergen as the main source (Figure 4). These observed patterns in genetic variation, structure, and connectivity suggest major anthropogenic impacts on the metapopulation dynamics and genetics of Svalbard reindeer.

Like Peary caribou, connectivity between island populations of Svalbard reindeer depends on sea ice corridors (Jenkins et al., 2016; Jenkins, Yannic, Schaefer, Conolly, & Lecomte, 2018). However, genetic differentiation in island populations of Peary caribou was largely explained by IBD as sea ice in the Canadian high Arctic has been relatively continuous in space and throughout the year (Comiso, Meier, & Gersten, 2017; Jenkins et al., 2016). Sea ice occurrence in coastal waters of Svalbard is more heterogeneous in time and space due to the inflow of warm Atlantic water in the west and cold Arctic water in the east. As our range-wide sampling covered this strong gradient in sea ice, we observed a marked IBR between natural sites, which explained more than three times the variation in genetic distance than IBD (Table 3). The strong genetic divergence and patterns of IBR also reflect the sedentary behavior of Svalbard reindeer (Côté et al., 2002; Hansen et al., 2010; Loe et al., 2016; Tyler & Øritsland, 1989). This is in sharp contrast with the migratory behavior of Peary caribou and other *Rangifer* (Jenkins et al., 2016; Miller et al., 2005), as well as the high dispersal capability of, for example, Arctic fox across sea ice (Ehrich, Carmichael, & Fuglei, 2012; Geffen et al., 2007).

The observed sea ice effect likely reflects both short- and long-term patterns of divergence, indirectly modified by past harvesting. Genetic differentiation depends on patch area and connectivity as well as the age of the population (Cosentino, Phillips, Schooley, Lowe, & Douglas, 2012) and colonization trajectories (Le Corre & Kremer, 1998). Therefore, genetic differentiation was likely weaker when reindeer could rely on dispersal across sea ice to recolonize patches where reindeer had been extirpated by harvesting, particularly in the east of Svalbard (e.g., from Edgeøya to Barentsøya; Norderhaug, 1970). However, less frequent sea ice and ice-covered fjords have likely led to greater divergence in recolonized locations along the west coast, and we even observed a tendency for an inverse relationship between genetic and geographic/ecological distance when accounting for reintroduction effects (Figure S6). Historical connectivity among remnant populations, particularly between Central Spitsbergen and the islands in East Svalbard, was evident from evolutionary estimates of gene flow (Figure 4). Genetic differentiation among extant populations has thus been influenced by sea ice connectivity and landscape barriers in the past. However, the observed source–sink dynamics are likely influenced by extirpations or quasi-extinctions from overharvesting if populations inhabiting the outer range experienced a slower recovery due to a harsher climate and/or prolonged bottleneck effects, such as increased genetic load (Kirkpatrick & Jarne, 2000). In addition, reduced gene flow as an indirect effect of overharvesting, that is, due to depleted source populations and extirpations of connecting patches, has likely contributed to the distinct genetic clustering and high F_{ST} values among the extant North Spitsbergen, Nordaustlandet, and East Svalbard populations.

Svalbard reindeer were assumed to be extirpated in South Spitsbergen before the 1820s, but this region was recently recolonized by a gradual southward expansion from Central Spitsbergen since the 1960s (Norderhaug, 1970). However, the low genetic diversity and the strong genetic differentiation between these two populations suggest that South Spitsbergen may have held a small remnant population after harvesting was banned. Nevertheless, continuous range expansion can result in a transient increase in population divergence and gradual loss of genetic diversity due to cumulative founder effects (Le Corre & Kremer, 1998). This is especially the case for expansions resembling a linear stepping-stone model as colonists are sampled from consecutively newly founded populations. The high Arctic muskox (*Ovibos moschatus*) experienced such a gradual decline in genetic diversity following successive colonizations of high Arctic Canadian islands and Greenland, leading to extremely high genetic differentiation among populations (Hansen et al., 2018). Hence, in Svalbard reindeer, a harvest-induced extirpation followed by successive founder events is the most logical explanation for the genetic signature in South Spitsbergen, especially considering the small available habitat patches and fragmented landscape along the southwest coast. A southward recolonization is also supported by the differential estimates of long-term gene flow (Figure 4) and most likely involved dispersal across ice-covered fjords in winter.

A similar southward expansion has occurred from the strongly divergent, remnant population in North Spitsbergen. However, a general lack of sea ice and ice-covered fjords in recent decades has prevented introgression with the reintroduced population in West Spitsbergen (Figures 1b and 2; Onarheim et al., 2014). Indeed, the naturally recolonized Mitrahalvøya is separated by merely 16 km of open water from the nearest reintroduced site, but F_{ST} values are as high as 0.41 (Table S3). Although reindeer are able swimmers, recolonizations of the peninsulas south of Ny-Ålesund and the easternmost island Prins Karls Forland were most likely mediated by dispersal across sea ice (Hansen et al., 2010). The genetic signature strongly supports the notion that reindeer would still have been extirpated in this region if they had not been reintroduced to Ny-Ålesund in the late 1970s. In comparison, introgression between two (or more) clusters mediated by dispersal across fjord ice was evident in both North Isfjorden and Wijdefjorden. The latter site in particular appears to be an important contact zone with elevated levels of genetic variability owing to strong divergence between the source (North Isfjorden and/or Central Spitsbergen) and recipient (North Spitsbergen) populations (see Maudet et al., 2002). This may explain why our analyses of recent gene flow failed to detect recent immigration to Wijdefjorden, but not to North Isfjorden (Table S7).

Today, Svalbard reindeer have recolonized their historical range, but recently recolonized populations are still recovering

from past overharvesting (Le Moullec et al., 2019). This ongoing extinction–colonization process is supported by the observed patterns of gene flow and strong genetic differentiation across the subspecies' distribution range. Furthermore, the effect of past harvesting through extirpations and reintroductions on the current metapopulation genetic structure was modified by recent loss of sea ice and reduced connectivity, restricting dispersal and gene flow. The strongest negative trends in Arctic sea ice have been observed around Svalbard and the northern Barents Sea (Comiso et al., 2017; Onarheim et al., 2014; Stroeve et al., 2007). Therefore, our study provides an early warning that continued sea ice decline linked to global warming will lead to increased genetic isolation and population differentiation through genetic drift, not only in Svalbard reindeer but also other Arctic wildlife, such as Peary caribou (Jenkins et al., 2016, 2018; Mallory & Boyce, 2019), Arctic fox (Geffen et al., 2007; Norén et al., 2011), polar bear (Laidre et al., 2018), and muskox (Hansen et al., 2018). Indeed, the populations of Svalbard reindeer that were reintroduced into West Spitsbergen are already facing increased demographic isolation due to sea ice loss (Nilsen et al., 2016; Pedersen et al., 2018), which increases their vulnerability to current climate change and the increased frequency of extreme winter weather events (Hansen, Aanes, Herfindal, Kohler, & Sæther, 2011; Peeters et al., 2019). Particularly rainy winters, causing extensive ice encapsulation of the tundra vegetation, usually occur over large areas and contribute to spatially synchronized population dynamics (Hansen et al., 2019; Peeters et al., 2019). Strong synchronization by climate is expected to increase the extinction risk of a metapopulation (Engen, Lande, & Sæther, 2002; Heino, Kaitala, Ranta, & Lindström, 1997). In Svalbard reindeer, the observed synchrony in short-term abundance fluctuations appears to be buffered by contrasting long-term trends in local abundances, linked to the spatial heterogeneity in climatic change effects (Hansen et al., 2019). Nevertheless, increased levels of inbreeding and the loss of genetic diversity are of great concern in small populations living at the outer limits of the distribution range, making them more vulnerable to extinction (Frankham, 1998; Saccheri et al., 1998). Future source–sink dynamics will likely be more characterized by dispersal across land and increased isolation of populations surrounded by the sea. Contact zones with high genetic mixture, such as Wijdefjorden, are therefore important focal populations for management and conservation. Further studies should implement modern genetic tools, such as SNPs or whole-genome sequencing, to detect local adaptation in small isolated populations and genome level changes under climate change.

ACKNOWLEDGEMENTS

We are indebted to Liv Midthjell for her technical help and guidance in the laboratory. Special thanks for collecting samples go to Morgan L. Bender, Christophe and Marie-Diane Vanquathem, Martin Kristiansen, Ragnhild Røsseland, Gard Christophersen, Bård Blæsterdalen, the Governor of Svalbard, and numerous field assistants. We thank the Norwegian Polar Institute and the University Centre of Svalbard for help with field logistics. We also thank Christophe Pelabon for critical feedback and Jos Milner for comments and language corrections. This study was funded by the Research Council of Norway through its Centre of Excellence (project 223257), KLIMAFORSK (244647), Arctic Field Grants (235652, 246054, and 257173), and INSYNC (276080), and by the Svalbard Environmental Protection Fund (projects 14/137 and 15/105) and the Norwegian Polar Institute.

CONFLICT OF INTEREST

We declare no conflicts of interest.

DATA AVAILABILITY STATEMENT

The data that support the findings of this study are available from the corresponding author upon reasonable request.

ORCID

Bart Peeters https://orcid.org/0000-0002-2341-1035
Mathilde Le Moullec https://orcid.org/0000-0002-3290-7091
Joost A. M. Raeymaekers https://orcid.org/0000-0003-2732-7495
Jonatan F. Marquez https://orcid.org/0000-0003-2034-6634
Vebjørn Veiberg https://orcid.org/0000-0003-1037-5183
Leif Egil Loe https://orcid.org/0000-0003-4804-2253
Brage B. Hansen https://orcid.org/0000-0001-8763-4361

REFERENCES

Aanes, R., Sæther, B.-E., & Øritsland, N. A. (2000). Fluctuations of an introduced population of Svalbard reindeer: The effects of density dependence and climatic variation. *Ecography*, *23*(4), 437–443. https://doi.org/10.1034/j.1600-0587.2000.230406.x

Albon, S. D., Irvine, R. J., Halvorsen, O., Langvatn, R., Loe, L. E., Ropstad, E., … Stien, A. (2017). Contrasting effects of summer and winter warming on body mass explain population dynamics in a food-limited Arctic herbivore. *Global Change Biology*, *23*(4), 1374–1389. https://doi.org/10.1111/gcb.13435

Allendorf, F. W., England, P. R., Luikart, G., Ritchie, P. A., & Ryman, N. (2008). Genetic effects of harvest on wild animal populations. *Trends in Ecology & Evolution*, *23*(6), 327–337. https://doi.org/10.1016/j.tree.2008.02.008

Alsos, I. G., Ehrich, D., Seidenkrantz, M.-S., Bennike, O., Kirchhefer, A. J., & Geirsdottir, A. (2016). The role of sea ice for vascular plant dispersal in the Arctic. *Biology Letters*, *12*(9), 20160264. https://doi.org/10.1098/rsbl.2016.0264

Alter, S. E., Rosenbaum, H. C., Postma, L. D., Whitridge, P., Gaines, C., Weber, D., … Hancock, B. L. (2012). Gene flow on ice: The role of sea ice and whaling in shaping Holarctic genetic diversity and population differentiation in bowhead whales (*Balaena mysticetus*). *Ecology and Evolution*, *2*(11), 2895–2911. https://doi.org/10.1002/ece3.397

Archer, F. I., Adams, P. E., & Schneiders, B. B. (2017). STRATAG: An R package for manipulating, summarizing and analysing population genetic data. *Molecular Ecology Resources*, *17*(1), 5–11. https://doi.org/10.1111/1755-0998.12559

Beerli, P. (2006). Comparison of Bayesian and maximum-likelihood inference of population genetic parameters. *Bioinformatics*, *22*(3), 341–345. https://doi.org/10.1093/bioinformatics/bti803

Beerli, P., & Felsenstein, J. (2001). Maximum likelihood estimation of a migration matrix and effective population sizes in n subpopulations by using a coalescent approach. *Proceedings of the National Academy*

of Sciences of the United States of America, *98*(8), 4563–4568. https://doi.org/10.1073/pnas.081068098

Calenge, C. (2006). The package "adehabitat" for the R software: A tool for the analysis of space and habitat use by animals. *Ecological Modelling*, *197*(3–4), 516–519. https://doi.org/10.1016/j.ecolmodel.2006.03.017

Chen, C., Durand, E., Forbes, F., & François, O. (2007). Bayesian clustering algorithms ascertaining spatial population structure: A new computer program and a comparison study. *Molecular Ecology Notes*, *7*(5), 747–756. https://doi.org/10.1111/j.1471-8286.2007.01769.x

Clarke, R. T., Rothery, P., & Raybould, A. F. (2002). Confidence limits for regression relationships between distance matrices: Estimating gene flow with distance. *Journal of Agricultural, Biological, and Environmental Statistics*, *7*(3), 361–372. https://doi.org/10.1198/108571102320

Comiso, J. C., Meier, W. N., & Gersten, R. (2017). Variability and trends in the Arctic Sea ice cover: Results from different techniques. *Journal of Geophysical Research-Oceans*, *122*(8), 6883–6900. https://doi.org/10.1002/2017jc012768

Cosentino, B. J., Phillips, C. A., Schooley, R. L., Lowe, W. H., & Douglas, M. R. (2012). Linking extinction–colonization dynamics to genetic structure in a salamander metapopulation. *Proceedings of the Royal Society B: Biological Sciences*, *279*(1733), 1575–1582. https://doi.org/10.1098/rspb.2011.1880

Côté, S. D., Dallas, J. F., Marshall, F., Irvine, R. J., Langvatn, R., & Albon, S. D. (2002). Microsatellite DNA evidence for genetic drift and philopatry in Svalbard reindeer. *Molecular Ecology*, *11*(10), 1923–1930. https://doi.org/10.1046/j.1365-294X.2002.01582.x

Coulon, A. (2010). Genhet: An easy-to-use R function to estimate individual heterozygosity. *Molecular Ecology Resources*, *10*(1), 167–169. https://doi.org/10.1111/j.1755-0998.2009.02731.x

Cronin, M. A., Patton, J. C., Balmysheva, N., & MacNeil, M. D. (2003). Genetic variation in caribou and reindeer (*Rangifer tarandus*). *Animal Genetics*, *34*(1), 33–41. https://doi.org/10.1046/j.1365-2052.2003.00927.x

Descamps, S., Aars, J., Fuglei, E., Kovacs, K. M., Lydersen, C., Pavlova, O., … Strøm, H. (2017). Climate change impacts on wildlife in a High Arctic archipelago – Svalbard, Norway. *Global Change Biology*, *23*(2), 490–502. https://doi.org/10.1111/gcb.13381

Do, C., Waples, R. S., Peel, D., Macbeth, G. M., Tillett, B. J., & Ovenden, J. R. (2014). NeEstimator v2: Re-implementation of software for the estimation of contemporary effective population size (Ne) from genetic data. *Molecular Ecology Resources*, *14*(1), 209–214. https://doi.org/10.1111/1755-0998.12157

Eckert, C. G., Samis, K. E., & Lougheed, S. C. (2008). Genetic variation across species' geographical ranges: The central-marginal hypothesis and beyond. *Molecular Ecology*, *17*(5), 1170–1188. https://doi.org/10.1111/j.1365-294X.2007.03659.x

Ehrich, D., Carmichael, L., & Fuglei, E. (2012). Age-dependent genetic structure of Arctic foxes in Svalbard. *Polar Biology*, *35*(1), 53–62. https://doi.org/10.1007/s00300-011-1030-1

Engen, S., Lande, R., & Sæther, B.-E. (2002). The spatial scale of population fluctuations and quasi-extinction risk. *American Naturalist*, *160*(4), 439–451. https://doi.org/10.1086/342072

Fay, F. H., Kelly, B. P., & Sease, J. L. (1989). Managing the exploitation of Pacific walruses: A tragedy of delayed response and poor communication. *Marine Mammal Science*, *5*(1), 1–16. https://doi.org/10.1111/j.1748-7692.1989.tb00210.x

Frankham, R. (1997). Do island populations have less genetic variation than mainland populations? *Heredity*, *78*, 311–327. https://doi.org/10.1038/hdy.1997.46

Frankham, R. (1998). Inbreeding and extinction: Island populations. *Conservation Biology*, *12*(3), 665–675. https://doi.org/10.1046/j.1523-1739.1998.96456.x

Frankham, R. (2005). Genetics and extinction. *Biological Conservation*, *126*(2), 131–140. https://doi.org/10.1016/j.biocon.2005.05.002

Geffen, E., Waidyaratne, S., Dalén, L., Angerbjörn, A., Vila, C., Hersteinsson, P., … Wayne, R. K. (2007). Sea ice occurrence predicts genetic isolation in the Arctic fox. *Molecular Ecology*, *16*(20), 4241–4255. https://doi.org/10.1111/j.1365-294X.2007.03507.x

Goudet, J. (2005). HIERFSTAT, a package for R to compute and test hierarchical F-statistics. *Molecular Ecology Notes*, *5*(1), 184–186. https://doi.org/10.1111/j.1471-8278.2004.00828.x

Governor of Svalbard. (2009). *Plan for the management of Svalbard reindeer, knowledge and management status* (Report No. 1/2009 in Norwegian). Longyearbyen, Norway: Governor of Svalbard.

Hansen, B. B., Aanes, R., Herfindal, I., Kohler, J., & Sæther, B.-E. (2011). Climate, icing, and wild arctic reindeer: Past relationships and future prospects. *Ecology*, *92*(10), 1917–1923. https://doi.org/10.1890/11-0095.1

Hansen, B. B., Aanes, R., & Sæther, B.-E. (2010). Partial seasonal migration in high-arctic Svalbard reindeer (*Rangifer tarandus platyrhynchus*). *Canadian Journal of Zoology*, *88*(12), 1202–1209. https://doi.org/10.1139/z10-086

Hansen, B. B., Pedersen, Å. Ø., Peeters, B., Le Moullec, M., Albon, S. D., Herfindal, I., … Aanes, R. (2019). Spatial heterogeneity in climate change effects decouples the long-term dynamics of wild reindeer populations in the high Arctic. *Global Change Biology*, *25*(11), 3656–3668. https://doi.org/10.1111/gcb.14761

Hansen, C. C. R., Hvilsom, C., Schmidt, N. M., Aastrup, P., Coeverden, V., de Groot, P. J., … Heller, R. (2018). The muskox lost a substantial part of its genetic diversity on its long road to Greenland. *Current Biology*, *28*(24), 4022–4028. https://doi.org/10.1016/j.cub.2018.10.054

Hanski, I. (1998). Metapopulation dynamics. *Nature*, *396*, 41–49. https://doi.org/10.1038/23876

Hardy, O. J., & Vekemans, X. (2002). SPAGeDi: A versatile computer program to analyse spatial genetic structure at the individual or population levels. *Molecular Ecology Notes*, *2*(4), 618–620. https://doi.org/10.1046/j.1471-8286.2002.00305.x

Heino, M., Kaitala, V., Ranta, E., & Lindström, J. (1997). Synchronous dynamics and rates of extinction in spatially structured populations. *Proceedings of the Royal Society B: Biological Sciences*, *264*(1381), 481–486. https://doi.org/10.1098/rspb.1997.0069

Higdon, J. (2010). Commercial and subsistence harvests of bowhead whales (*Balaena mysticetus*) in eastern Canada and West Greenland. *Journal of Cetacean Research and Management*, *11*(2), 185–216.

Jenkins, D. A., Lecomte, N., Schaefer, J. A., Olsen, S. M., Swingedouw, D., Côté, S. D., … Yannic, G. (2016). Loss of connectivity among island-dwelling Peary caribou following sea ice decline. *Biology Letters*, *12*(9), 20160235. https://doi.org/10.1098/rsbl.2016.0235

Jenkins, D. A., Yannic, G., Schaefer, J. A., Conolly, J., & Lecomte, N. (2018). Population structure of caribou in an ice-bound archipelago. *Diversity and Distributions*, *24*(8), 1092–1108. https://doi.org/10.1111/ddi.12748

Johansen, B. E., Karlsen, S. R., & Tømmervik, H. (2012). Vegetation mapping of Svalbard utilising Landsat TM/ETM plus data. *Polar Record*, *48*(244), 47–63. https://doi.org/10.1017/s0032247411000647

Kalinowski, S. T. (2005). HP-RARE 1.0: A computer program for performing rarefaction on measures of allelic richness. *Molecular Ecology Notes*, *5*(1), 187–189. https://doi.org/10.1111/j.1471-8286.2004.00845.x

Kirkpatrick, M., & Jarne, P. (2000). The effects of a bottleneck on inbreeding depression and the genetic load. *The American Naturalist*, *155*(2), 154–167. https://doi.org/10.1086/303312

Kruse, F. (2017). Catching up: The state and potential of historical catch data from Svalbard in the European Arctic. *Polar Record*, *53*(5), 520–533. https://doi.org/10.1017/S0032247417000481

Kvie, K. S., Heggenes, J., Anderson, D. G., Kholodova, M. V., Sipko, T., Mizin, I., & Røed, K. H. (2016). Colonizing the high Arctic: Mitochondrial DNA reveals common origin of Eurasian archipelagic reindeer (*Rangifer tarandus*). *PLoS ONE*, *11*(11), e0165237. https://doi.org/10.1371/journal.pone.0165237

Laidre, K. L., Born, E. W., Atkinson, S. N., Wiig, Ø., Andersen, L. W., Lunn, N. J., … Heagerty, P. (2018). Range contraction and increasing isolation of a polar bear subpopulation in an era of sea-ice loss. *Ecology and Evolution*, *8*(4), 2062–2075. https://doi.org/10.1002/ece3.3809

Lande, R. (1998). Anthropogenic, ecological and genetic factors in extinction and conservation. *Researches on Population Ecology*, *40*(3), 259–269. https://doi.org/10.1007/bf02763457

Latch, E. K., Dharmarajan, G., Glaubitz, J. C., & Rhodes, O. E. (2006). Relative performance of Bayesian clustering software for inferring population substructure and individual assignment at low levels of population differentiation. *Conservation Genetics*, *7*(2), 295–302. https://doi.org/10.1007/s10592-005-9098-1

Le Corre, V., & Kremer, A. (1998). Cumulative effects of founding events during colonisation on genetic diversity and differentiation in an island and stepping-stone model. *Journal of Evolutionary Biology*, *11*(4), 495–512. https://doi.org/10.1046/j.1420-9101.1998.11040495.x

Le Moullec, M., Pedersen, Å. Ø., Stien, A., Rosvold, J., & Hansen, B. B. (2019). A century of conservation: The ongoing recovery of Svalbard reindeer. *The Journal of Wildlife Management*, *83*(8), 1676–1686. https://doi.org/10.1002/jwmg.21761

Leblond, M., St-Laurent, M.-H., & Côté, S. D. (2016). Caribou, water, and ice – fine-scale movements of a migratory arctic ungulate in the context of climate change. *Movement Ecology*, *4*(1), 14. https://doi.org/10.1186/s40462-016-0079-4

Lefcheck, J. S. (2016). piecewiseSEM: Piecewise structural equation modelling in R for ecology, evolution, and systematics. *Methods in Ecology and Evolution*, *7*(5), 573–579. https://doi.org/10.1111/2041-210X.12512

Loe, L. E., Hansen, B. B., Stien, A., D. Albon, S., Bischof, R., Carlsson, A., … Mysterud, A. (2016). Behavioral buffering of extreme weather events in a high-Arctic herbivore. *Ecosphere*, *7*(6), e01374. https://doi.org/10.1002/ecs2.1374

Lønø, O. (1959). *The reindeer on Svalbard* (report series no. 83 in Norwegian). Oslo, Norway: Norwegian Polar Institute.

Luximon, N., Petit, E. J., & Broquet, T. (2014). Performance of individual vs. group sampling for inferring dispersal under isolation-by-distance. *Molecular Ecology Resources*, *14*(4), 745–752. https://doi.org/10.1111/1755-0998.12224

Mallory, C. D., & Boyce, M. S. (2019). Prioritization of landscape connectivity for the conservation of Peary caribou. *Ecology and Evolution*, *9*(4), 2189–2205. https://doi.org/10.1002/ece3.4915

Mantel, N. (1967). Detection of disease clustering and a generalized regression approach. *Cancer Research*, *27*, 209–220.

Maudet, C., Miller, C., Bassano, B., Breitenmoser-Wursten, C., Gauthier, D., Obexer-Ruff, G., … Luikart, G. (2002). Microsatellite DNA and recent statistical methods in wildlife conservation management: Applications in Alpine ibex *Capra ibex* (*ibex*). *Molecular Ecology*, *11*(3), 421–436. https://doi.org/10.1046/j.0962-1083.2001.01451.x

McRae, B. H. (2006). Isolation by resistance. *Evolution*, *60*(8), 1551–1561. https://doi.org/10.1111/j.0014-3820.2006.tb00500.x

McRae, B. H., & Beier, P. (2007). Circuit theory predicts gene flow in plant and animal populations. *Proceedings of the National Academy of Sciences of the United States of America*, *104*(50), 19885–19890. https://doi.org/10.1073/pnas.0706568104

Miller, D. L., Burt, M. L., Rexstad, E. A., & Thomas, L. (2013). Spatial models for distance sampling data: Recent developments and future directions. *Methods in Ecology and Evolution*, *4*(11), 1001–1010. https://doi.org/10.1111/2041-210X.12105

Miller, F. L., Barry, S. J., & Calvert, W. A. (2005). Sea-ice crossings by caribou in the south-central Canadian Arctic Archipelago and their ecological importance. *Rangifer*, *25*(4), 77–88. https://doi.org/10.7557/2.25.4.1773

Nilsen, F., Skogseth, R., Vaardal-Lunde, J., & Inall, M. (2016). A simple shelf circulation model: Intrusion of Atlantic water on the West Spitsbergen shelf. *Journal of Physical Oceanography*, *46*(4), 1209–1230. https://doi.org/10.1175/jpo-d-15-0058.1

Norderhaug, M. (1970). *The Svalbard reindeer in the 1960's* (report series no. 99 in Norwegian). Oslo, Norway: Norwegian Polar Institute.

Norén, K., Carmichael, L., Fuglei, E., Eide, N. E., Hersteinsson, P., & Angerbjörn, A. (2011). Pulses of movement across the sea ice: Population connectivity and temporal genetic structure in the arctic fox. *Oecologia*, *166*(4), 973–984. https://doi.org/10.1007/s00442-011-1939-7

Nychka, D., Furrer, R., Paige, J., & Sain, S. (2017). *fields: Tools for spatial data* (R package version 9.6). Retrieved from https://doi.org/10.5065/D6W957CT

Oksanen, J., Blanchet, F. G., Friendly, M., Kindt, R., Legendre, P., McGlinn, D., … Wagner, H. (2018). *vegan: Community ecology package* (*R-package version 2.5-2*). Retrieved from https://CRAN.R-project.org/package=vegan

Onarheim, I. H., Smedsrud, L. H., Ingvaldsen, R. B., & Nilsen, F. (2014). Loss of sea ice during winter north of Svalbard. *Tellus A: Dynamic Meteorology and Oceanography*, *66*(1), 23933. https://doi.org/10.3402/tellusa.v66.23933

Pedersen, Å. Ø., Hansen, B. B., Loe, L. E., Ropstad, E., Irvine, R. J., Stien, A., & Ravolainen, V. (2018). *When ground-ice replaces fjord-ice – Results from a study of GPS-collared Svalbard reindeer females* (brief report no. 49). Tromsø, Norway: Norwegian Polar Institute.

Peeters, B., Pedersen, Å. Ø., Loe, L. E., Isaksen, K., Veiberg, V., Stien, A., … Hansen, B. B. (2019). Spatiotemporal patterns of rain-on-snow and basal ice in high Arctic Svalbard: Detection of a climate-cryosphere regime shift. *Environmental Research Letters*, *14*(1), 015002. https://doi.org/10.1088/1748-9326/aaefb3

Peterman, W. E. (2018). ResistanceGA: An R package for the optimization of resistance surfaces using genetic algorithms. *Methods in Ecology and Evolution*, *9*(6), 1638–1647. https://doi.org/10.1111/2041-210X.12984

Petersen, S. D., Manseau, M., & Wilson, P. J. (2010). Bottlenecks, isolation, and life at the northern range limit: Peary caribou on Ellesmere Island. *Canada. Journal of Mammalogy*, *91*(3), 698–711. https://doi.org/10.1644/09-mamm-a-231.1

Pinsky, M. L., & Palumbi, S. R. (2014). Meta-analysis reveals lower genetic diversity in overfished populations. *Molecular Ecology*, *23*(1), 29–39. https://doi.org/10.1111/mec.12509

Post, E., Bhatt, U. S., Bitz, C. M., Brodie, J. F., Fulton, T. L., Hebblewhite, M., … Walker, D. A. (2013). Ecological consequences of sea-ice decline. *Science*, *341*(6145), 519–524. https://doi.org/10.1126/science.1235225

Post, E., Forchhammer, M. C., Bret-Harte, M. S., Callaghan, T. V., Christensen, T. R., Elberling, B., … Aastrup, P. (2009). Ecological dynamics across the Arctic associated with recent climate change. *Science*, *325*(5946), 1355–1358. https://doi.org/10.1126/science.1173113

Pritchard, J. K., Stephens, M., & Donnelly, P. (2000). Inference of population structure using multilocus genotype data. *Genetics*, *155*(2), 945–959.

Prop, J., Aars, J., Bårdsen, B.-J., Hanssen, S. A., Bech, C., Bourgeon, S., … Moe, B. (2015). Climate change and the increasing impact of polar bears on bird populations. *Frontiers in Ecology and Evolution*, *3*, 33. https://doi.org/10.3389/fevo.2015.00033

R Core Team. (2016). *R: A language and environment for statistical computing*. Vienna, Austria: R Foundation for Statistical Computing. Retrieved from http://www.R-project.org/

Røed, K. H. (2003). Refugial origin and postglacial colonization of holarctic reindeer and caribou. *Rangifer*, *25*(1), 19–30. https://doi.org/10.7557/2.25.1.334

Rousset, F. (1997). Genetic differentiation and estimation of gene flow from F-statistics under isolation by distance. *Genetics*, *145*(4), 1219–1228.

Rousset, F. (2000). Genetic differentiation between individuals. *Journal of Evolutionary Biology*, *13*(1), 58–62. https://doi.org/10.1046/j.1420-9101.2000.00137.x

Saccheri, I., Kuussaari, M., Kankare, M., Vikman, P., Fortelius, W., & Hanski, I. (1998). Inbreeding and extinction in a butterfly metapopulation. *Nature*, *392*(6675), 491–494. https://doi.org/10.1038/33136

Serreze, M. C., Barrett, A. P., Stroeve, J. C., Kindig, D. N., & Holland, M. M. (2009). The emergence of surface-based Arctic amplification. *Cryosphere*, *3*(1), 11–19. https://doi.org/10.5194/tc-3-11-2009

Stien, A., Bårdsen, B.-J., Veiberg, V., Andersen, R., Loe, L. E., & Pedersen, Å. Ø. (2012). *Hunting on Svalbard reindeer – Knowledge status and evaluation of relevant management models* (Report to Svalbard Environmental Protection Fund, in Norwegian). Longyearbyen, Norway: Governor of Svalbard.

Storfer, A., Murphy, M. A., Spear, S. F., Holderegger, R., & Waits, L. P. (2010). Landscape genetics: Where are we now? *Molecular Ecology*, *19*(17), 3496–3514. https://doi.org/10.1111/j.1365-294X.2010.04691.x

Stroeve, J., Holland, M. M., Meier, W., Scambos, T., & Serreze, M. (2007). Arctic sea ice decline: Faster than forecast. *Geophysical Research Letters*, *34*(9), L09501. https://doi.org/10.1029/2007gl029703

Taylor, S. S., Jenkins, D. A., & Arcese, P. (2012). Loss of MHC and neutral variation in Peary caribou: Genetic drift is not mitigated by balancing selection or exacerbated by MHC allele distributions. *PLoS ONE*, *7*(5), e36748. https://doi.org/10.1371/journal.pone.0036748

Tyler, N. J. C., & Øritsland, N. A. (1989). Why don't Svalbard reindeer migrate? *Holarctic Ecology*, *12*(4), 369–376. https://doi.org/10.1111/j.1600-0587.1989.tb00911.x

Van Etten, J. (2017). R package gdistance: Distances and routes on geographical grids. *Journal of Statistical Software*, *76*(13), 1–21. https://doi.org/10.18637/jss.v076.i13

Vuilleumier, S., Bolker, B. M., & Leveque, O. (2010). Effects of colonization asymmetries on metapopulation persistence. *Theoretical Population Biology*, *78*(3), 225–238. https://doi.org/10.1016/j.tpb.2010.06.007

Walsh, P. S., Metzger, D. A., & Higuchi, R. (1991). Chelex 100 as a medium for simple extraction of DNA for PCR-based typing from forensic material. *BioTechniques*, *10*(4), 506–513.

Waples, R. S., & Do, C. (2010). Linkage disequilibrium estimates of contemporary Ne using highly variable genetic markers: A largely untapped resource for applied conservation and evolution. *Evolutionary Applications*, *3*(3), 244–262. https://doi.org/10.1111/j.1752-4571.2009.00104.x

Weir, B. S., & Cockerham, C. C. (1984). Estimating F-statistics for the analysis of population structure. *Evolution*, *38*(6), 1358–1370. https://doi.org/10.2307/2408641

Wilson, G. A., & Rannala, B. (2003). Bayesian inference of recent migration rates using multilocus genotypes. *Genetics*, *163*(3), 1177–1191.

Yannic, G., Ortego, J., Pellissier, L., Lecomte, N., Bernatchez, L., & Côté, S. D. (2017). Linking genetic and ecological differentiation in an ungulate with a circumpolar distribution. *Ecography*, *41*(6), 922–937. https://doi.org/10.1111/ecog.02995

Yannic, G., Pellissier, L., Ortego, J., Lecomte, N., Couturier, S., Cuyler, C., … Côté, S. D. (2014). Genetic diversity in caribou linked to past and future climate change. *Nature Climate Change*, *4*, 132–137. https://doi.org/10.1038/nclimate2074

Yannic, G., St-Laurent, M.-H., Ortego, J., Taillon, J., Beauchemin, A., Bernatchez, L., … Côté, S. D. (2016). Integrating ecological and genetic structure to define management units for caribou in Eastern Canada. *Conservation Genetics*, *17*(2), 437–453. https://doi.org/10.1007/s10592-015-0795-0

SUPPORTING INFORMATION

Additional supporting information may be found online in the Supporting Information section.

How to cite this article: Peeters B, Le Moullec M, Raeymaekers JAM, et al. Sea ice loss increases genetic isolation in a high Arctic ungulate metapopulation. *Glob Change Biol*. 2020;26:2028–2041. https://doi.org/10.1111/gcb.14965